We are IntechOpen, the world's leading publisher of Open Access books Built by scientists, for scientists

4,800
Open access books available

122,000
International authors and editors

135M
Downloads

Our authors are among the

154
Countries delivered to

TOP 1%
most cited scientists

12.2%
Contributors from top 500 universities

CLARIVATE ANALYTICS
BOOK CITATION INDEX
INDEXED

WEB OF SCIENCE™

Selection of our books indexed in the Book Citation Index
in Web of Science™ Core Collection (BKCI)

Interested in publishing with us?
Contact book.department@intechopen.com

Numbers displayed above are based on latest data collected.
For more information visit www.intechopen.com

Effect of the Processing Conditions on the Microstructural Features and Mechanical Behavior of Aluminum Alloys

Tomasz Tański and Przemysław Snopiński

Additional information is available at the end of the chapter

Abstract

Aluminum and aluminum alloys are widely used for aircraft structures, where they are subjected to demanding conditions and where is an increased demand for weight reduction and fuel savings. Aluminum comprises 8% of the earth's crust and is, therefore, the most abundant structural metal. Its production since 1965 has surpassed that of copper and now comes next to iron. This increased use of aluminum alloys leads to a need for deeper understanding of their mechanical properties and the impacts of processing parameters. The mechanical properties can determine by controlling the microstructures of the alloys. For example, precipitation hardening is the main strengthening mechanism improving the tensile and yield strength. Solute atoms, precipitates and dispersoids influences to the yield strength, since they act as distributed pinning points for mobile dislocations, thus increasing the shear stress required to move the dislocations. Another approach is the manipulation of a grain size that can be performed by alloying or plastic deformation processes. Therefore, the precise understanding of each mechanism that can influence the properties of aluminum and its alloys is very important. The aim of this chapter is to shed light on the influence of the processing history on the microstructure and mechanical properties.

Keywords: aluminum, heat treatment, structure, properties, severe plastic deformation

1. Aluminum—introduction

Aluminum is the third most abundant element in the earth's crust and the most abundant metallic element. For the last five decades, it has been second only to iron in an industrial use. It is worth to point out that the potential of aluminum as engineering material was found well before it became an industrial material. It was supposed that the most useful field for this metal will be in its alloys. At the beginning, the application of aluminum was limited to small- or

high-valuable items due to the very high cost of this material. Nowadays, pure aluminum and its alloys play a fundamental role in engineering. Aluminum is the most heavily consumed non-ferrous metal in the world, with concurrent annual production at 130 million metric tonnes. About 50% of this total alumina production ~65 million tonnes is "primary aluminum". The process of primary aluminum production is divided into three separate stages [1–3].

- Mining of the raw material (bauxite and a variety of ores);
- Preparation of an aluminum oxides from ores;
- Production of primary aluminum.

The total world production of primary aluminum has increased from 13 million metric tones in 1974 to about 65 million metric tones in 2016 (**Figure 1**).

At present, consumers and engineers are demanding energy efficiency, thus aluminum can play a fundamental role in driving this change. Due to the fact that by replacing the steel parts with those made from aluminum, a significant decrease in weight can be achieved, many car
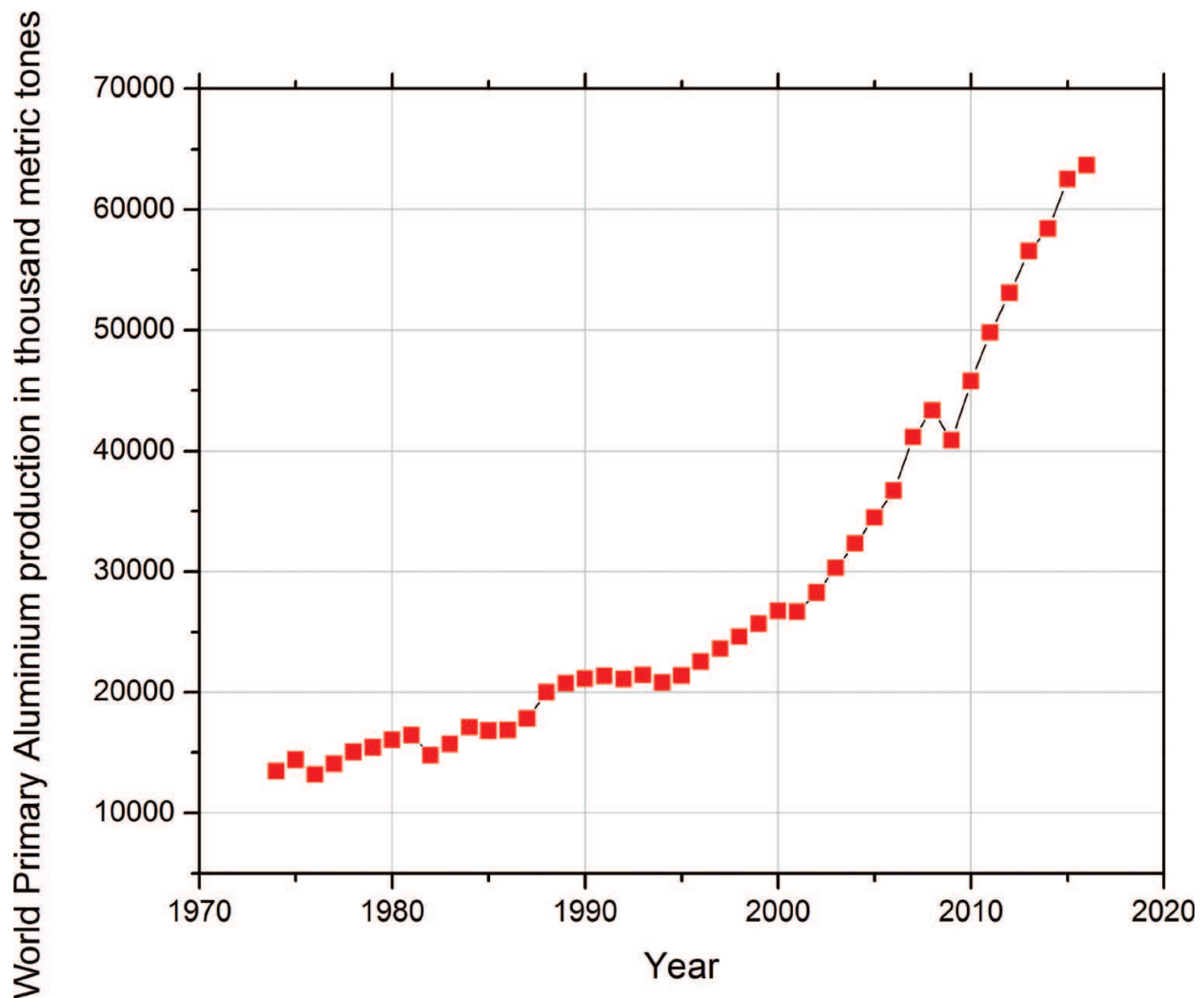

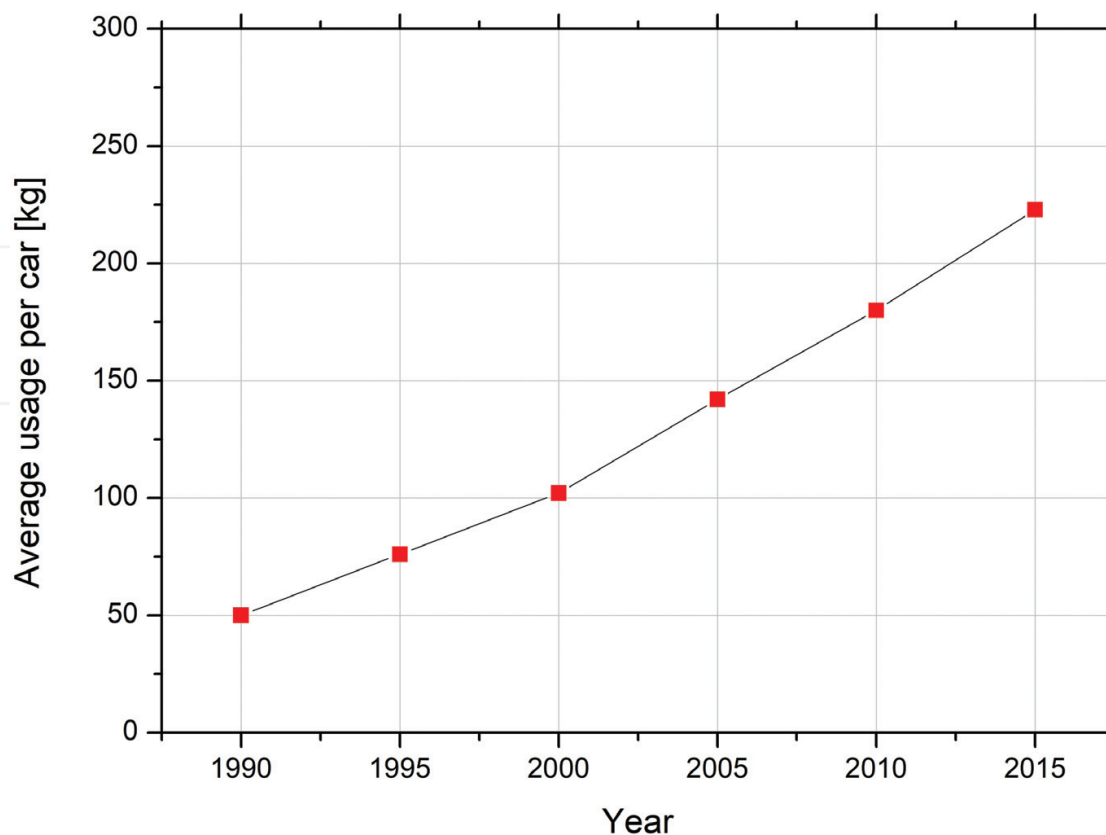**Figure 1.** World primary aluminum production [4].

Figure 2. Average use of aluminum per car—data in Western Europe [5].

companies are now moving to aluminum to achieve this goal. Moreover, its usage in the automotive industry is accelerating (**Figure 2**) because it offers the fastest, safest and environmentally friendly way to increase performance and fuel economy. Aluminum and its alloys are mainly used in an automotive, aerospace and construction engineering due to their unique properties such as corrosion resistance and high specific strength. Its usage in automotive applications has increased by more than 80% in the past 5 years. It is predicted that a total amount of about 50 kg of aluminum content per car produced in Europe in 1990 will increase to about 250 kg in the 2020 year. However, to meet the engineers' demand, the properties of Al and its alloys have to be increased or modified, which can be obtained through the microalloying, heat treatment, plastic deformation or the combination of this treatment [2, 3, 6].

2. Strengthening of aluminum

Like all known pure metals, in comparison to its alloys, pure aluminum has a low strength. Therefore, many elements are added to solid solution of aluminum. All known alloying elements that are used for the production of Al alloys can be classified into three principal groups: basic, ancillary additions and impurities. Depending upon the nature of an alloy, the same elements could play different roles. In a great majority of aluminum alloys, four kinds of alloying elements are used: magnesium, zinc, copper and silicon. These additions can be

classified as "basic" or "principal", due the fact that they are introduced into Al solid solution in (relatively) large amounts and create their microstructure mechanical and physical properties. This introduction of relatively large amounts of alloying elements can be done because they are characterized by considerable solubility in Al. Due this fact this introduced atoms are obstacles for dislocation movement and enhances strength. The solid solution strengthening can take place through three basic mechanisms:

- Lattice strain field interactions between dislocations and alloying atoms result in a decrease of dislocation movement.

- Alloying elements that are in solid solution impose lattice strains on surrounding host atoms.

- Alloying atoms tend to diffuse and segregate around the dislocation to find atomic sites more suited to their radii. This decreases the entire strain energy and "anchor" or "pin" the dislocation.

The final properties of such alloys depend on a complex interaction of chemical composition, solidification sequence of main phases during crystallization process history [1, 6–10].

The most important function of the alloying of Al solid solution is to enhance alloy mechanical properties. A strengthening effect proceeds when lattice strain field interactions occur between alloying elements and dislocations. These dislocations are imperfections in the atomic structure of the material. This single atom can substitute the aluminum atoms in the lattice. In addition, they may fit in the atomic lattice being substitutional atoms (**Figure 3**). In contrast to
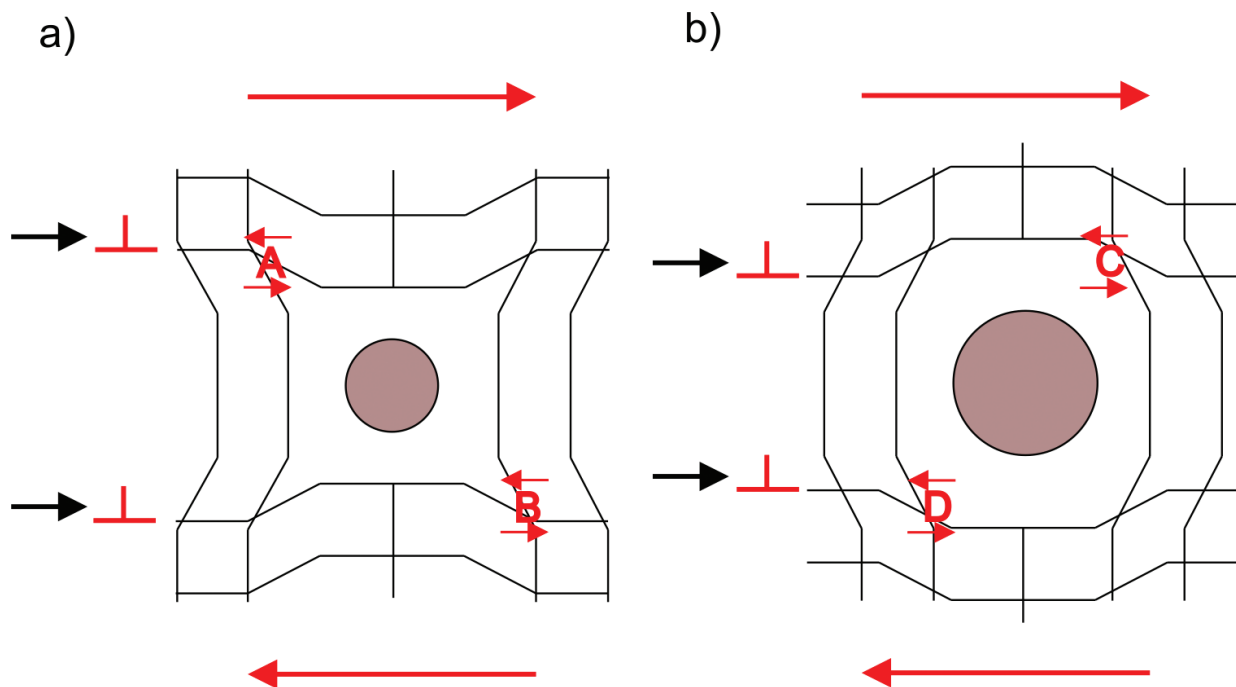

Figure 3. The principle of solid solution strengthening mechanism due atomic radii mismatch, (a) smaller substitutional alloying element generates a local shear at A and B that opposes motion of dislocation to the right, (b) element generates a local shear at C and D that opposes motion of dislocation to the right [9].

substitutional atoms, the interstitial atoms have considerably smaller atomic radii than aluminum. Due to the fact that aluminum has a small atomic radii, the interstitial atoms do not frequently form substitutional atoms. Atoms introduced to the aluminum lattice can cause a distortion in crystal lattice and these distorted regions impede the dislocation movement which causes a strengthening effect. The difference of the Al atomic radii and that used in alloying element ((RAl − R2)/RAl) × 100% reach the maximal value, for instance for magnesium (11.7%) and copper (10.5%). These alloying elements provide the greatest solid solution strengthening effect ($\Delta\sigma_b$/1 at.% = 30–40 MPa). The addition of alloys in aluminum may also influence other important properties such as castability. This property, to a very significant extent, will define whether an alloy could be used in industry or not [6–10]. For most engineering parts made from aluminum two types of alloys are used:

• Non-heat-treatable or work-hardening that are solid solution (and eventually strain) hardened, showing a good combination of strength and formability.

• The heat-treatable alloys that obtain their required strength through the heat treatment— (precipitation treatment).

The mechanical properties of Al alloys can also be enhanced by the formation of fine uniformly dispersed in Al matrix particles of the second phase within the original phase matrix. This process is known as precipitation (age) hardening. The fundamental demand for an alloy to be strengthened through this process is that solid solubility decrease with decreasing temperature. The age hardening of Al alloys is accomplished by two individual heat treatments. At the first stage, a material is subjected to a solution heat treatment in which all of the β phases dissolves and forms a single-phase solid solution. Moreover, in a great majority of Al alloys, the diffusion rates are very slow for this reason the solution treatment has to be conducted for relatively long periods. The solution treatment is followed by rapid quenching. At this stage of heat treatment, a non-equilibrium situation exists in which α phase solid solution with some atoms of an alloying element is present. The alloy in this state is weak and ductile. To achieve the strengthening effect, the second type of treatment must be used—aging. At this stage, the supersaturated solid solution is heated to an intermediate temperature, at which diffusion rates become appreciable. The secondary β phase precipitate start to form as fine dispersed particles in a specified precipitation sequence that may consist of the coherent, semicoherent and non-coherent precipitates. The character, coherence and subsequently the strength depend on the temperature and time of artificial aging and a lattice misfit between a strengthening precipitate and Al matrix. The strength enhancement is reached because dislocations interact with these precipitates. Depending on the character of a precipitate and crystallographic orientation in relation with an aluminum matrix, different interactions can occur. Precipitates can be impenetrable or penetrable by dislocations. In the first case, a dislocation is forced by the applied stress bow around the precipitate and bypasses it, leaving a dislocation loop around the particle which is called Orowan loop (**Figure 4**). In the second case, the precipitate can be sheared by the dislocations and moves through the crystal. This phenomenon can occur when the precipitate is coherent with the Al matrix. Generally, coherent particles can be penetrable or not, while large particles are usually incoherent thus impenetrable. For some Al alloys such as Al-Cu, precipitation strengthening can occur spontaneously at room
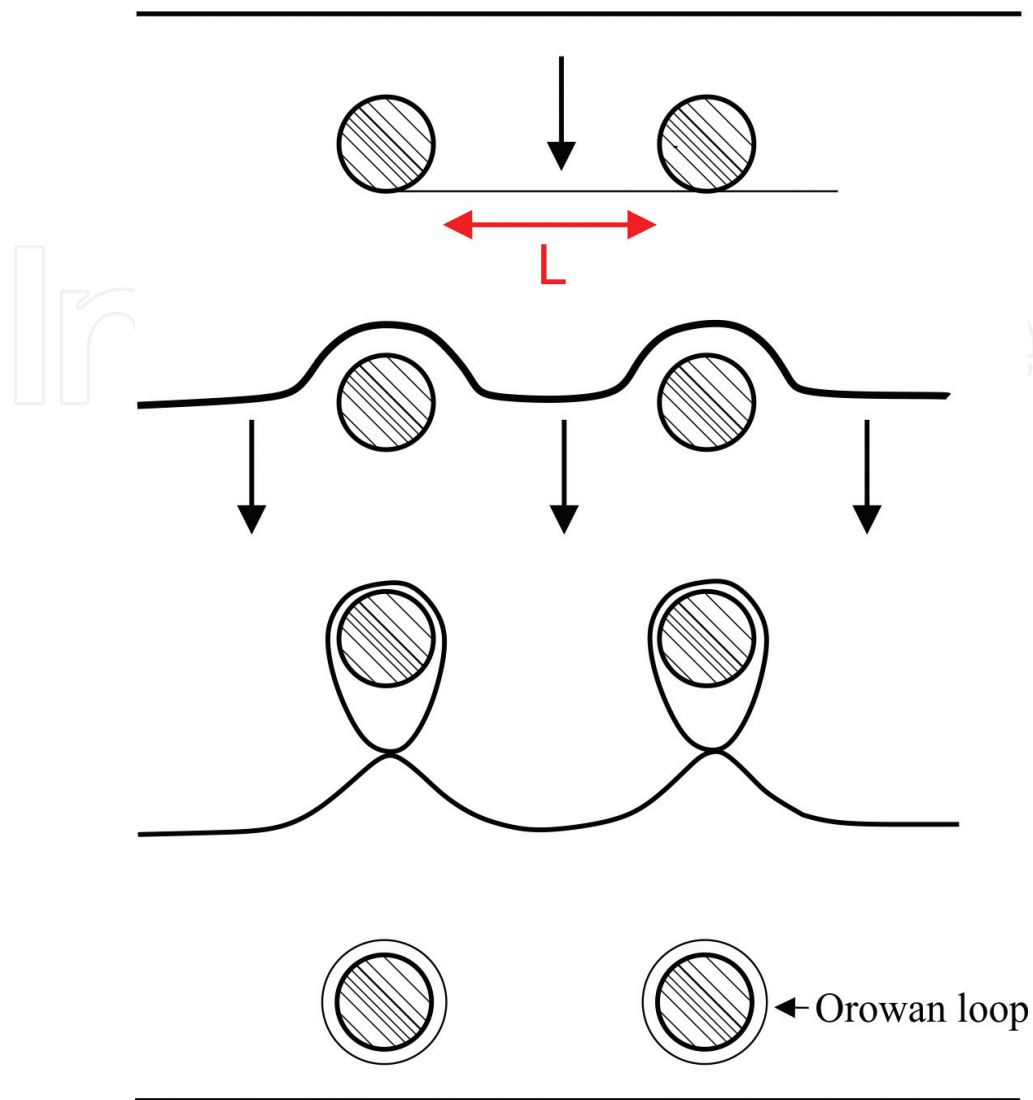
Figure 4. Dislocation bypass by the Orowan bowing mechanism [8].

temperature over long time periods. The growth of mechanical properties during natural aging is continuous or becomes stable. Whereas in artificially aged alloy with an increase in aging time, the strength of the material reaches a maximum value, and after that diminishes. This decrease of mechanical strength is known as overaging and usually can be related to a growth of precipitates and coherency loss [7–13].

Another principal tool used for strength enhancement of many materials is the manipulation of their grain size. When the material is deformed and when the resistance to plastic flow is governed by dislocation glide and diffusion-controlled processes are not an issue, a decrease in the grain size causes the strengthening effect [14–17]. Thus, the mechanical strength is related to the grain size, d, through the Hall-Petch equation which states that the yield stress, σ_y is given by:

$$\sigma_y = \sigma_0 + k_y d^{-1/2} \tag{1}$$

To transform a coarse-grained microstructure into an ultrafine, it is required to impose an exceptionally high strain into a sample to introduce a high density of dislocations and to allow

these dislocations to re-arrange to form an array of grain boundaries—usually the low-angle grain boundaries are transformed into a high-angle grain. The conventional metal-working procedures, such as drawing, extrusion, rolling or forging, are restricted in their ability to produce ultrafine grains for two important reasons. First, there is a limitation on the overall strain that may be imposed using these procedures because the processing techniques incorporate corresponding reductions in the cross-sectional dimensions of the work-pieces. The second reason is that the strains imposed in conventional processing are insufficient to convert coarsely grained structures into this ultra fine-grained (UFG) because most of the industrially used alloys exhibit low workability at ambient and low temperatures. As a consequence of the limitations mentioned above, attention has been paid to develop an alternative metal-working procedure, based on the application of severe plastic deformation (SPD) techniques, where a sample is subjected to the extremely high strains which are imposed at relatively low temperatures without changing cross-sectional dimensions of the samples. Many different SPD techniques are now available and summaries of these various procedures published in works of many scientists are in this several reviews [14–18]. Nevertheless, major emphasis has been placed to date on the two techniques of equal channel angular pressing (ECAP) and high pressure torsion (HPT) and, accordingly, one of these procedures—ECAP will be used in this report.

3. Principles and processing by ECAP

There are numerous studies showing the behavior of aluminum alloys samples subjected to a severe plastic strain [12–18], including metal processing through the standard industrial methods of rolling or extrusion, but all of these processes necessitate a change in the dimensions of the work samples. In contrast to these methods, ECAP processing differs from them. The general principle of ECAP procedure is shown schematically in **Figure 5**.

Processing by ECAP uses a specially designed die consisting of two channels that are bent through a sharp angle near the die center. The sample is usually pre-machined to fit tight the channel, and then is pressed through die using a plunger. The ECAP die is defined by two angles: the channel angle Φ that represents the intersection angle of two parts of the channel, and second is the curvature angle Ψ that represents the angle at the outer arc of curvature where the two parts of the channel intersect. The cross-sectional dimensions of the work sample are not changed during processing thus the process can be repeated to obtain high strain accumulation. Additionally, it is possible to initiate different slip systems by sample rotation between consecutive passes. This processing routes are termed in nomenclature as route A where the sample is pressed repetitively without rotation, routes B_A and B_C where the sample is rotated by 90° along the longitudinal axis in alternate direction and same direction, respectively, and route C where the sample is rotated by 180° between each passes. The equivalent strain imposed in one pass of ECAP is dependent primarily upon the die channel angle Φ and, to a lesser extent, on the angle Ψ. It can be shown from first principles that the shear strain ε_N is given by a relationship of the form [14–20].

$$\varepsilon_N = \frac{N}{\sqrt{3}}\left[2\,cot\left(\frac{\Phi}{2}+\frac{\Psi}{2}\right)+\Psi\,cos\left(\frac{\Phi}{2}+\frac{\Psi}{2}\right)\right] \qquad (2)$$
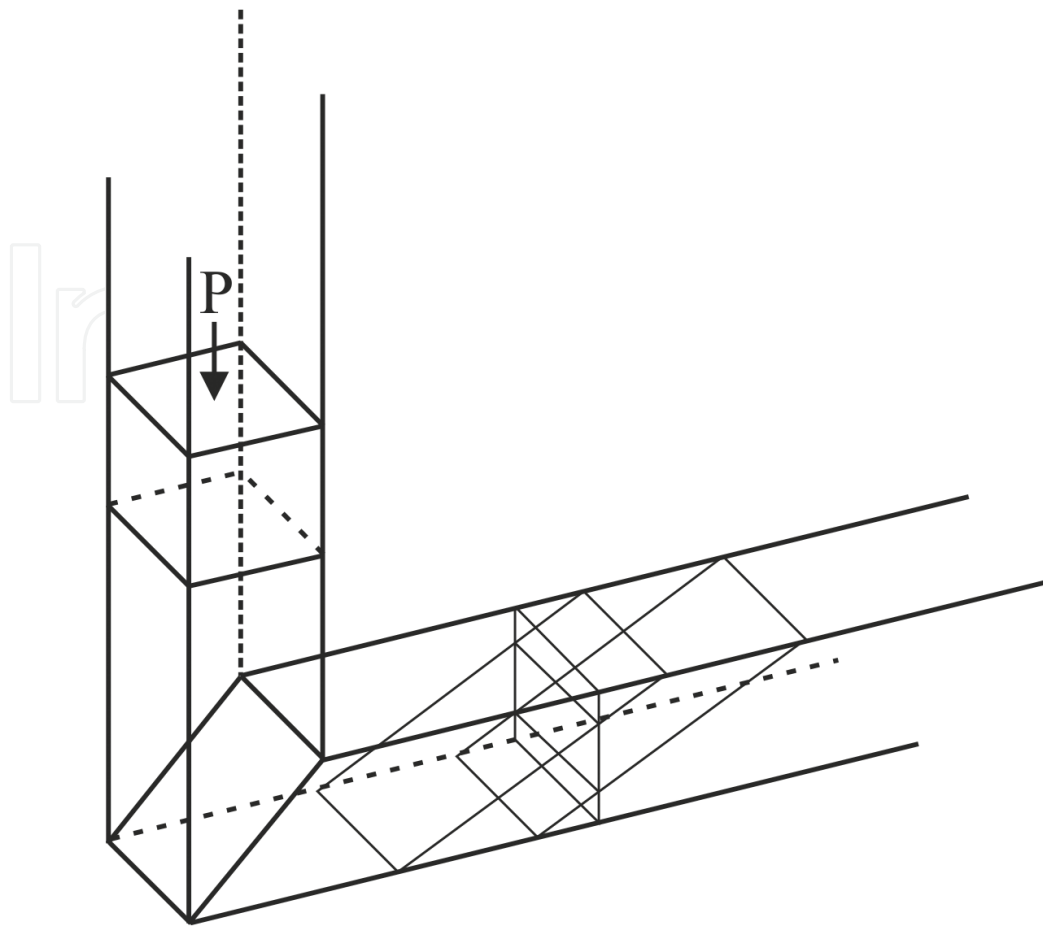
Figure 5. The general principle of ECAP processing [14].

where N is the number of ECAP passes. In conventional ECAP, it is generally assumed that the billet fills the corner of the die at the intersection of the two parts of the channel, and this produces a uniform microstructure throughout the billet.

4. Aluminum-magnesium alloys

Al-Mg alloys are commonly used in transport and for structural components in the automotive industry due to their combination of good properties that are excellent corrosion and high specific strength. As of now, mechanical properties and corrosion resistance of Al-Mg alloys are required to be improved to broaden the application area in a new industrial field. It is well known that the great mechanical properties of Al-Mg alloys come from magnesium solution strengthening. The solubility of magnesium in aluminum is very high ~14.9% at 450°C (**Figure 6**) thus alloying even with small quantity of Mg, results in a significant increase in strength due the solution strengthening [21–26].

With an increase in Mg content, Al-Mg alloys become susceptible to intergranular corrosion thus their application field is limited. This susceptibility to corrosion is due to the formation of anodic β (Al$_3$Mg$_2$) phase at grain boundaries. Due the fact that the β phase is strongly anodic
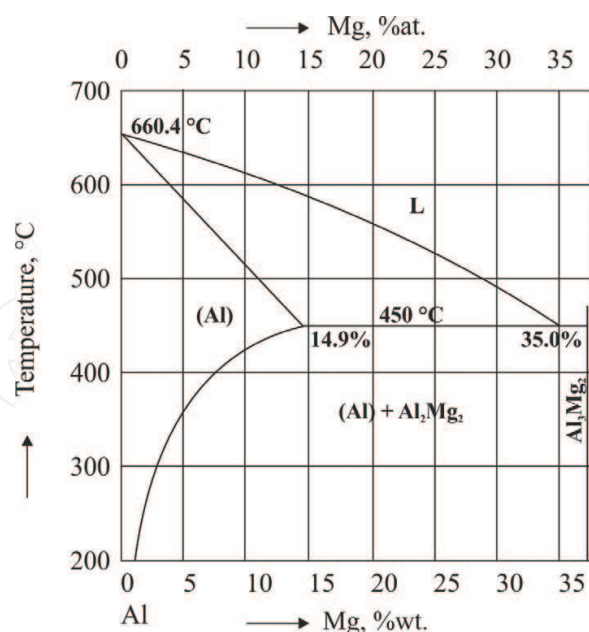
Figure 6. Aluminum-magnesium binary diagram [11].

in relation to the Al matrix, it corrodes and dissolves very fast when alloy is exposed to a conductive medium such as seawater. This is because of the formation of galvanic coupling between the Al matrix and the β phase. The dissolution of continuous grain boundary β phase results in the decrease in the bond strength of grain boundaries, and leads to elements failure. The size, morphology and its distribution were reported to be affected by a heat treatment conditions. It was found that precipitation of β phase at the grain boundaries increases with time of heat treatment at an elevated temperature. The precipitation velocity of β-Al_3Mg_2 phase can be controlled by temperature. Precipitation of β phase can be continuous at 160°C, but at higher temperature of annealing (220°C) becomes discontinuous. The formation of β′ and β phase is associated with the change in mechanical properties during the heat treatment. Recently, more details of the precipitation process in Al-Mg alloys, such as the lattice structure, limited formation temperatures and shape of different precipitates were obtained from many investigation results [21–26].

Based on the data published in the nomenclature, the precipitation sequence [27–31] in Al-Mg alloys can be described as follows:

$$\text{Supersaturated solid solution-GP zone} - \beta'' - \beta' - \beta \text{ phase} \qquad (3)$$

where GP (Guinier-Preston) zones (short-range ordered Al_3Mg) have a modulated structure and β″ phase (long-range ordered Al_3Mg, a = 0.408 nm) has an L12 structure in which Al and Mg atoms are alternatively aligned along the [100] directions. β′ phase, Al_3Mg_2, is reported to have a hexagonal (a = 1.002 nm, c = 1.636 nm) structure and semi-coherent with the matrix. The equilibrium β phase, Al_3Mg_2, is of fcc structure (a = 2.824 nm) with a unit cell containing 1186 atoms. However, the precipitation sequence can be slightly changed if aging temperature or Mg content is different.

5. Material and experimental procedure

The chemical composition of the aluminum-magnesium alloy used in this investigation is given in **Table 1**.

Mg	Fe	Si	Cu	Ti	Al
2.86	0.07	0.07	0.01	0.01	Rest

Table 1. Chemical composition of AlMg3 aluminum alloys/wt.%.

The first stage of the experiment was to investigate the aging behavior of the solution-treated samples. The process was conducted in a resistance furnace followed by quenching and artificial aging. To characterize mechanical properties and investigate the aging response, hardness measurements were performed using Rockwell hardness tester ZWICK ZHR 4150. For selected samples, the static tensile tests were also performed. In the second stage, samples were subjected to the ECAP process. Two different dies were used in this investigation. First $\Phi = 120°$, providing an equivalent strain equal to ~0.6 in each pass and second $\Phi = 90°$ with an additional twist angle at the outer channel providing an equivalent strain ~1. To decrease the friction MoS_2 was used as a coating lubricant. For a metallographic study, samples were prepared according to Struers standards. To reveal structure constituents, samples were etched using Keller's, Weck's and Barker's reagent. The microstructure was characterized with an Axio Observer Image Analyzer light microscope under bright field and polarized light. To obtain information about the chemical composition of the precipitates, scanning electron microscope equipped with an energy-dispersive X-ray spectroscopy (EDS) detector was used. The examinations of the thin foils microstructure and phase identification were made on the high-resolution transmission electron microscope JEM 3010UHR from JEOL, at an accelerating voltage of 200 kV.

6. Results

6.1. Structure

The representative structures of the Al-Mg alloy are presented in **Figure 7a–c**. It can be visible that as-cast microstructure can be characterized as fine dendritic. Moreover, in the interdendritic regions, β-Al_3Mg_2 phase exists and are visible insoluble inclusions of the Si- and Fe-rich phases. Precipitation treatment led to the disappearance of the fine dendritic microstructure and has no significant impact on the grain size. An EDS chemical composition microanalysis presented in **Table 2** and **Figure 8** allow one to confirm the presence of the main structure constituents. However, due to the fact that expected size of the strengthening precipitates is >200 nm, the EDS analysis can be overestimated. Therefore, to identify the morphology and crystal structure of precipitates, transmission electron microscopy (TEM) was used (**Figure 9a–e**). It is clear, that during the precipitation treatment process from supersaturated solid solution, the hardening secondary phases β'-Al_3Mg_2 precipitates [32]. This secondary precipitate, of which average diameter was measured to be approximately
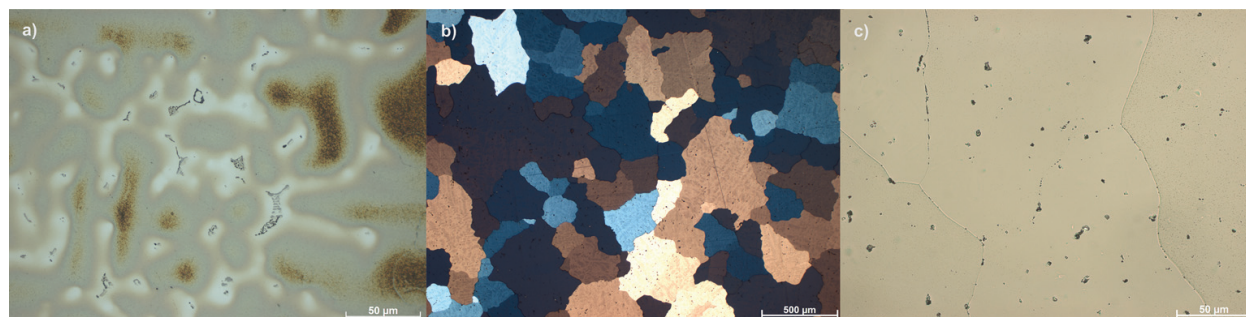
Figure 7. Microstructures of AlMg3 alloy (a) as-cast state (Weck's reagent), (b) precipitation-treated state (Barker's reagent)—polarized light, (c) precipitation-treated (Keller's reagent).

Point/phase	Element/line	The average mass concentration of elements (%)	
		Weight (%)	Atomic (%)
1/Mg$_2$Si	MgK	56.46	59.84
	AlK	5.74	5.48
	SiK	37.81	34.68
2/Al$_3$Fe	AlK	54.45	71.22
	FeK	45.55	28.78

Table 2. Results of pointwise EDS chemical composition microanalysis.

~100 nm (**Figure 9a**) in the nomenclature is known as metastable with a hexagonal crystal structure (a = 1.002 nm, c = 1.636 nm), semi-coherent to the aluminum matrix. The β′ precipitates are formed mainly through nucleation and growth on the structural defects of the matrix. Moreover, it can be also observed that after precipitation treatment, Al$_3$Fe and Mg$_2$Si phases are still present which confirms the presented TEM study. Al$_3$Fe impurities precipitates are usually formed after annealing at 550°C and can pin down the dislocation motion while at lower temperature Al$_6$Fe forms. Next, to the small Al$_3$Fe phase, larger—about 2 μm in length —Mg$_2$Si precipitate with many dislocations around can be observed (**Figure 9b**).

In this study, Rockwell hardness measurements were used as an initial assessment of the influence heat treatment conditions on the mechanical properties. The experimental results permitted a correlation between hardness, microstructure and heat treatment conditions to be established. The mechanical test results are summarized and listed in **Tables 3** and **4**. Solution treatment temperature was selected to be just below the solidus temperature (based on the Al-Mg binary diagram—**Figure 6**). In this study, the temperature of artificial aging was selected to be 160 and 180°C, respectively. Based on the data listed in **Tables 3** and **4**, it can be concluded that the AlMg3 alloy exhibits a high aging potential. It can be observed that there is a 50% increase in hardness of heat-treated samples. Taking into account the energy costs, the most beneficial conditions seem to be solution treatment and artificial aging for 8 h while the temperature has minor influence on the strength. The observed increase in hardness is a result
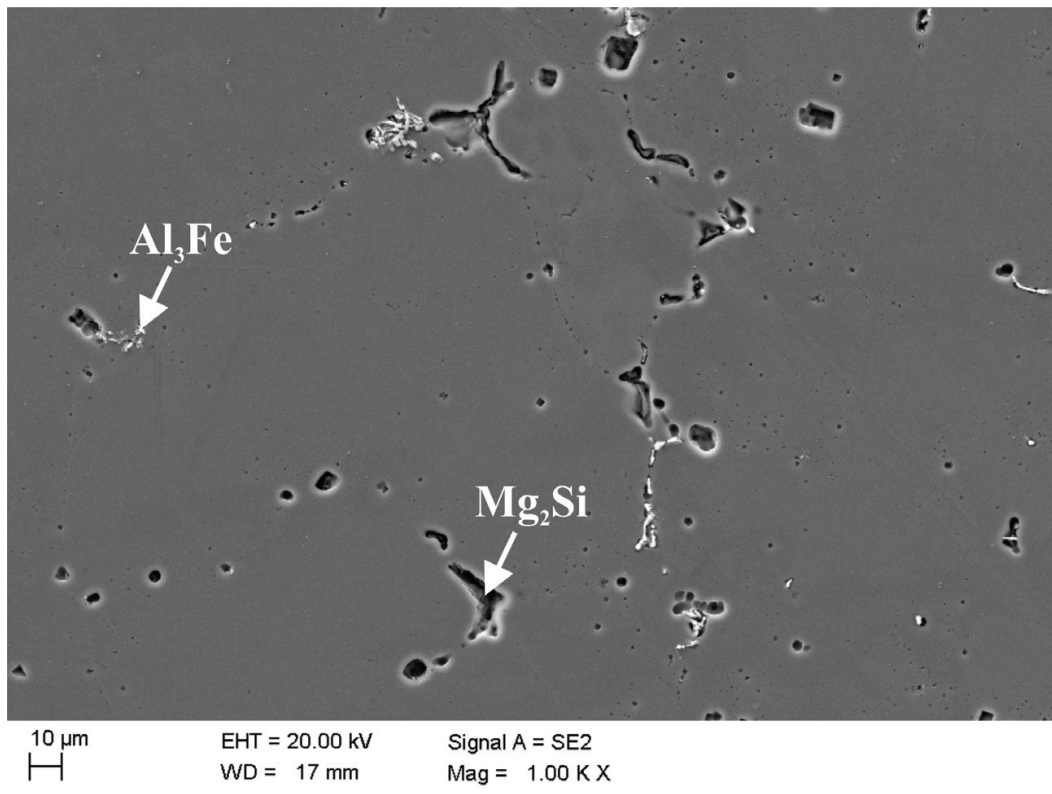
Figure 8. The SEM microstructure of AlMg3 alloy in precipitation-treated state.
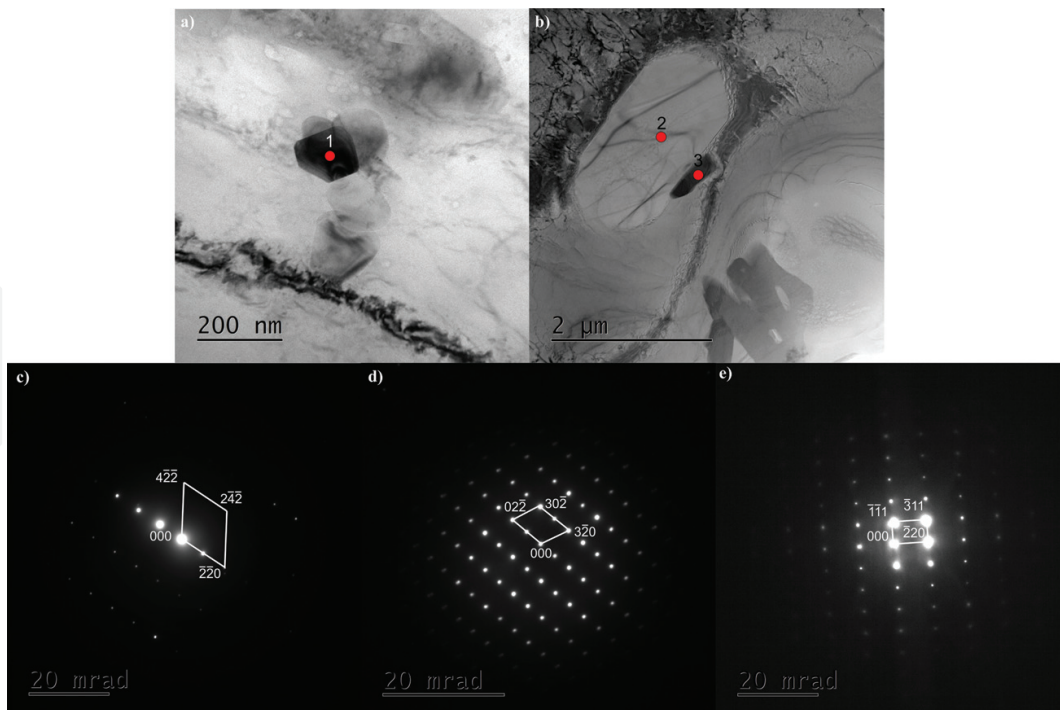

Figure 9. TEM microstructures of the AlMg3 alloy in precipitation-treated state showing size and morpholohgy of (a) β′-Al₃Mg₂ hardenning phase, (b) Mg₂Si and Al₃Fe phases, (c) diffraction spot from point 1 (Al₃Mg₂), (d) diffraction spot from point 2 (Mg₂Si) and (e) diffraction spot from point 3 (Al₃Fe).

Solution treatment conditions		Artificial aging time (h) (160°C)											
Temp. (°C)	Time (h)	0	4	8	12	0	4	8	12	0	4	8	12
		Hardness (HRF)				Tensile strength (MPa)				Elongation at failure (%)			
580	8	45	65	63	66	198	224	232	236	29	30	25	26
	12	46	68	69	67	197	214	225	233	29	29	28	27

Table 3. Summary of the mechanical properties of AlMg3 alloy aged at 160°C.

Solution treatment conditions		Artificial aging time (h) (160°C)											
Temp. (°C)	Time (h)	0	4	8	12	0	4	8	12	0	4	8	12
		Hardness (HRF)				Tensile strength (MPa)				Elongation at failure (%)			
580	8	45	65	63	66	198	222	236	232	29	28	26	23
	12	46	68	69	67	197	234	238	225	29	25	24	23

Table 4. Summary of the mechanical properties of AlMg3 alloy aged at 180 °C.

of the precipitation of the semicoherent secondary $\beta' - Al_3Mg_2$ phase from the supersaturated solid solution sssα [33, 34].

To examine the influence of the selected heat treatment conditions on the tensile properties, static tensile tests were carried out. It can be concluded from the presented data that in both investigated cases an increase in tensile strength is quite similar. **Tables 3** and **4** show the relationship between the tensile strength and heat treatment conditions. The values of the tensile strength slightly increase with aging time. Aging at higher temperature increases the tensile strength more rapidly. Tensile strength reaches the maximum after 12 h of artificial aging (at 160°C) and 8 hours (at 180°C). However, when the sample is aged at 180°C for 12 h, a decrease in ultimate tensile strength is observed—sample is overaged. Time of solution treatment has a minor influence on the mechanical properties. Additionally, in contrast to the tensile strength, the values of elongation at failure decreases with time. When the temperature of artificial aging is lower (160°C), the values of elongation decreases slightly from 29% (solution-treated sample) to about 25%. While aging at 180°C decreases elongation to about 23%. This is due to the fact that higher aging temperature increases the rate of the precipitation process which enhances the mechanical properties but on the other hand decreases the ductility.

6.2. Severe plastic deformation

Figure 10a illustrates the evolution of the microstructure of the Al-3%Mg alloy subjected to six ECAP passes followed by a precipitation treatment. Based on the metallographic analysis, it can be concluded that the individual grains cannot be clearly distinguished. The grains become elongated due to the imposed shear strain. Slip, shear and micro-shear bands create the band-like microstructure. These bands also refine microstructure of the Al-3%Mg alloy. Moreover, it can be observed that deformation bands have a preferred crystallographic orientation. In addition, each single shear or micro-shear band causes lattice rotations lying within the
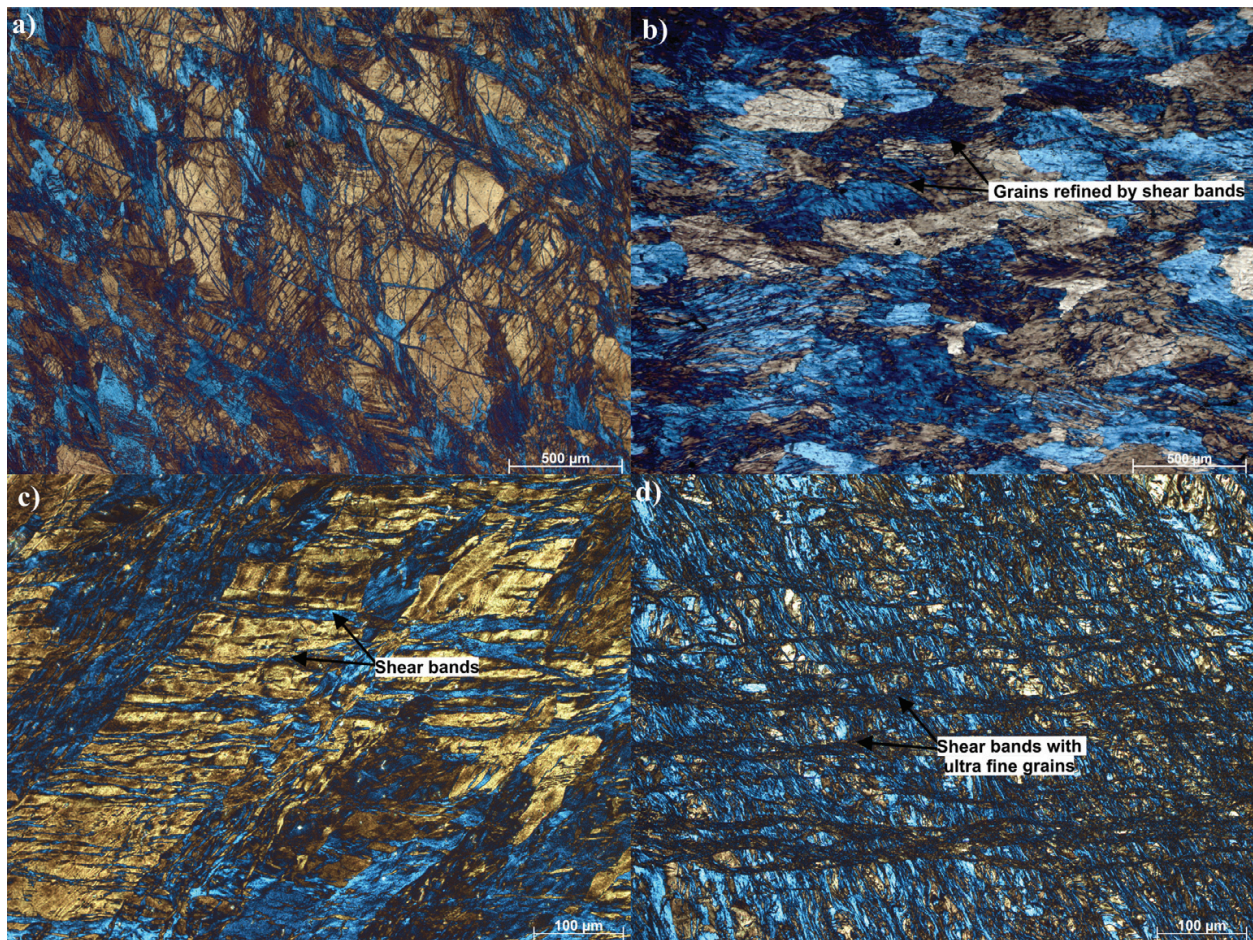
Figure 10. Optical microscope microstructures of the AlMg3 alloy (a) precipitation treated +6 ECAP passes (120°die, route B_c), (b) initial state +1 ECAP pass (90° die with 30° twist, route A), (c) initial state +2 ECAP passes (90° die with 30° twist, route A), (d) initial state +4 ECAP passes (90° die with 30° twist, route A).

low-to-moderate grain/(sub)grain boundary misorientation and thus their interactions can result in a violent appearance of the deformation bands having high-angle misorientations. Moreover, it can also be visible that the microstructure consists of the regions with the higher density of deformation bands and those less affected. This is due to the fact that, during shear deformation in the ECAP process, individual grains in the work samples cannot be deformed uniformly because of the orientation difference. **Figure 10b–d** illustrates the microstructure evolution of AlMg3 aluminum alloy subjected to the ECAP with a modified die. It can be observed that the obtained microstructures differ from that obtained using the conventional equipment. The grains in the microstructure after one ECAP pass are elongated, parallel to the transverse direction (TD), while when the number of ECAP passes increases, the obtained microstructures becomes more complex. It can be seen in **Figure 6c** (two ECAP passes) that additional shear is introduced by the twist angle—shear bands intersect at an angle of about 60° after two ECAP passes (there is an extra shear after each pass at an angle of 30°). When a number of accumulated strain increases to about ~4 (**Figure 10d**)—four ECAP passes, the microstructure looks as completely refined. There is no possibility to distinguish the individual grains. Due to this fact, to study the changes in the microstructure at higher magnification, TEM study was used.

The microstructures of the as deformed (FCC) metals are very complex. The size of individual grains differs thus grains with diversified size may coexist. Different structure constituents, such as dislocation-free grains, non-equilibrium grain boundaries, dislocation cell and (sub) grain structures, low-angle GBs (LAGBs), high-angle grain boundaries (HAGBs), stacking faults (SFs) and nanotwins, can also be identified [15–22, 33–36]. **Figure 11a** shows the typical microstructure of the as deformed material where a dislocation forest forms dense dislocation walls (DDWs). These DDWs forming cell blocks are free from dislocations. The size of cell blocks is about 1 μm. One of the most substantial characteristics of the microstructure after
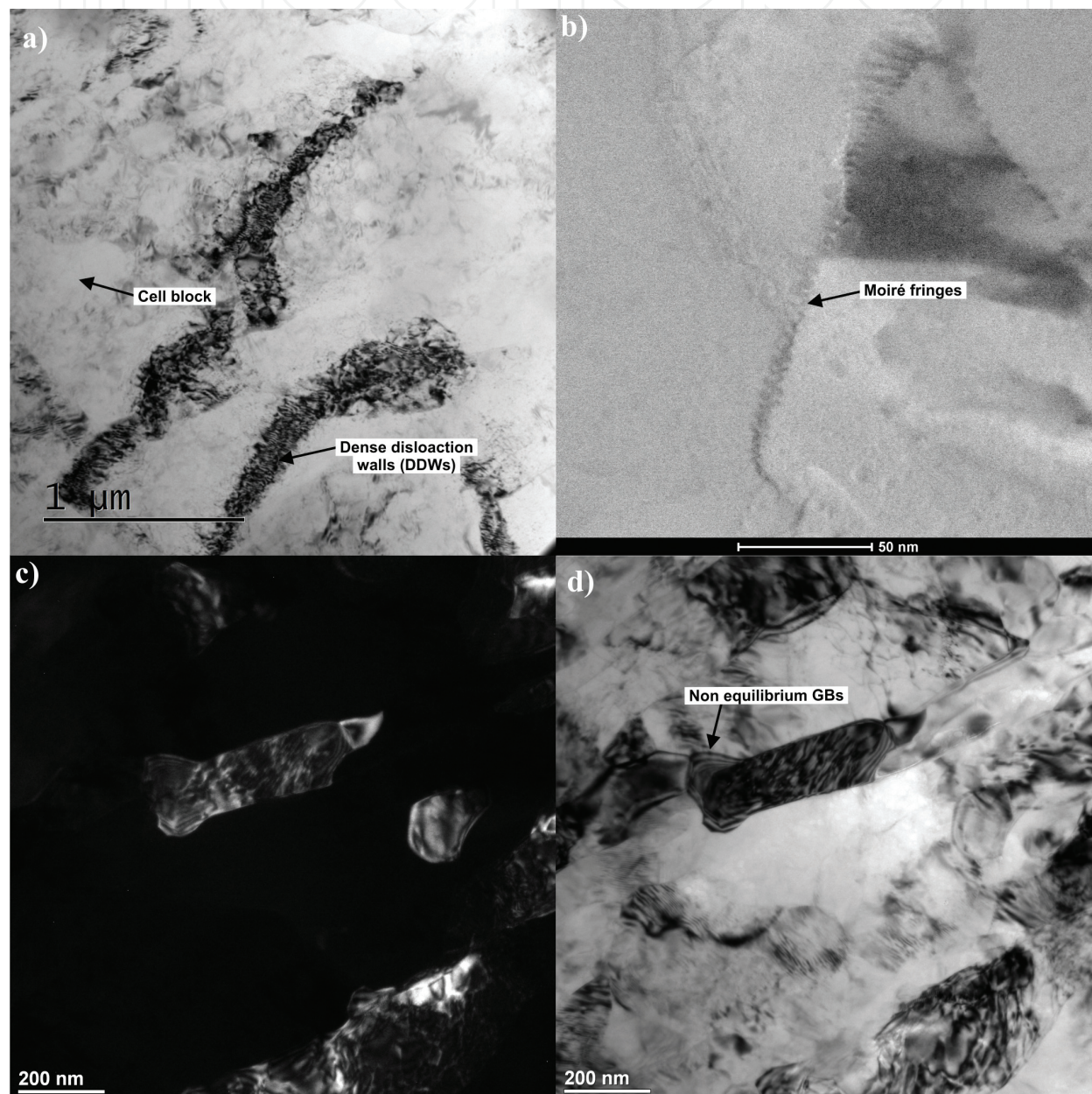

Figure 11. Bright field TEM images showing general microstructure of AlMg3 alloy (a) and (b) bright filed TEM images showing microstructure of AlMg3 alloy—precipitation treated and six ECAP passes, (c) dark field TEM image of AlMg3 alloy—four ECAP passes (90° die with 30° twist, route A), (d) bright field TEM image from the same area.

SPD processing is that some grain boundaries may give the appearance of extinction contours. The presence of diffuse grain boundaries is due the introduction of non-equilibrium grain boundaries having an excess extrinsic dislocations. This indicates the presence of high internal stresses and elastic distortions in the crystal lattice. It has been also suggested that these non-equilibrium GBs may have a strong effect on grain boundary processes such as sliding or diffusion. One can also see dislocation tangles in the grain interiors which can be considered as early stages of dislocation cell structure formation. This is related to an increase of strain accumulation in the material after the consecutive passes of ECAP process. Moreover, the presented TEM investigation results indicate that some grain interiors may also be free from dislocations and the dislocation density varies from crystallite to crystallite. Some grains also have sharp boundaries and are completely free of dislocations and no (sub)grains or dislocation cells can be observed in these grains. Such straight and narrow grain boundaries are believed to be in an equilibrium state and are high-angle grain boundaries (HAGBs). TEM investigation has also revealed the presence of Moiré fringes (**Figure 11b**). Early formation of very low-angle boundaries—typically for $\varphi < 2°$, is usually reported in the nomenclature by an existence of Moiré fringes. This also indicates that lamellar dislocation and cell boundaries continuously form during ECAP process. **Figure 11c** and **d** shows dark field and bright field images of AlMg3 alloy in as-cast state subjected to four passes using a modified die. It is clearly visible that with an increase in the number of ECAP passes, the grain/subgrain size decreases while the dislocation accumulation rise.

To evaluate the influence of the severe plastic deformation process using ECAP method of samples subjected to different strain paths, hardness measurements and tensile properties were determined. Due to the small sample size obtained from modified ECAP equipment, determination of the tensile properties was not possible. The effects of a number of passes and used ECAP die on mechanical properties are summarized in **Table 5**.

It is obvious that the plastic deformation processes result in increase strength, however, processing by SPD allows to impose much greater amounts of plastic strain in comparison to the conventional processes. Based on the data analysis presented in **Table 5**, it can be observed that there is a significant increase in the tensile properties of the $6\times$ ECAPed sample (about 50% in comparison to a precipitation-treated state). This growth of mechanical properties may be

	Hardness (Hv$_{0.3}$)	Ultimate tensile strength (MPa)	Elongation at failure (%)
As-cast	45	198	31
Precipitation treated	65	232	25
Precipitation treated + 6 ECAP passes (120° die)	126	384	2.4
As-cast + 1 ECAP pass (90° die, 30° twist)	95	—	—
As-cast + 2 ECAP passes (90° die, 30° twist)	107	—	—
As-cast + 3 ECAP passes (90° die, 30° twist)	112	—	—
As-cast + 4 ECAP passes (90° die, 30° twist)	120	—	—

Table 5. Summary of the mechanical properties of AlMg3 alloy in different states.

attributed to the accumulation of many excess dislocations generated through dislocation multiplication during ECAP by a volume fraction of the grain boundaries in the fine-grained microstructure. However, it can also be seen that the material after SPD processing loses its ductility rapidly. The processing using a modified ECAP die also results in a significant increase in hardness which grows gradually with an increase in ECAP cycles. This considerable strength increase may be attributed to three strengthening mechanisms, that is, solution strengthening, dislocation strengthening and grain size strengthening. Solution strengthening originates from the elastic distortions, however, the dislocation strengthening and grain refinement strengthening are the main contributors to the significant strength increase of AlMg3 alloy.

7. Conclusions

In this study, we investigate the effect of an ECAP die, its modification and combination of this process with a heat treatment with the aim to estimate the influence of process parameters on the structural evolution and mechanical properties of the AlMg3 aluminum alloy. Based on the analysis of the obtained results, the following conclusions can be stated.

The microstructure of the Al-3%Mg alloy in a precipitation-treated state consists of the α-Al matrix, large precipitates of Mg_2Si, Al_3Fe phases and β'-Al_3Mg_2 fine precipitates with hexagonal structure. The presence of a β'-Al_3Mg_2 phase causes a strengthening effect.

The mechanism of the microstructure refinement after the ECAP process consists of the creation of dislocation cell structures, non-equilibrium grain boundaries, (sub)grain boundaries and HAGBs. (Sub)grains develop from dislocation cells. The refined microstructure consists of the areas with deformation bands (shear bands) separated by HAGBs and non-refined regions with LAGBs and very low-angle boundaries (showing Moiré fringes on TEM). It is believed that the grain boundaries first transform into LAGBs and finally HAGBs with an increase in plastic strain accumulation.

The evolution of hardness of AlMg3 alloy when processed by ECAP with modified die shows a significant increase after the first pass followed by a more gradual increase with subsequent pressings until a saturated value is achieved after ~four ECAP passes.

The improved mechanical properties of the AlMg3 aluminum alloy obtained through the combination of ECAP process with heat treatment were a consequence of the solid solution strengthening, precipitation hardening and grain refinement.

Author details

Tomasz Tański* and Przemysław Snopiński

*Address all correspondence to: tomasz.tanski@polsl.pl

Silesian University of Technology, Gliwice, Poland

References

[1] Bloeck M. 5 - Aluminium sheet for automotive applications, In Advanced Materials in Automotive Engineering, edited by Jason Rowe, Woodhead Publishing, Sawston, Cambridge UK. 2012, P. 85-108, ISBN 9781845695613

[2] De Matteis G, Brando G, Mazzolani FM. Pure aluminium: An innovative material for structural applications in seismic engineering. Construction and Building Materials. 2012; **26**:677-686

[3] Miller WS, Zhuang L, Bottema J, Wittebrood AJ, De Smet P, Haszler A, Vieregge A. Recent development in aluminium alloys for the automotive industry. Materials Science and Engineering A. 2000;**280**:37-49

[4] http://www.world-aluminium.org/statistics/alumina-production/

[5] http://www.totalmateria.com/page.aspx?ID=CheckArticle&site=ktn&NM=137

[6] shby MF, Jones DRH. Engineering Materials 1 - An Introduction to their Properties & Applications. Linacre House, UK/Woburn, MA, USA: Butterworth-Heinemann An imprint of Elsevier Science; 1996. p. 1-322

[7] Zolotorevsky VS, Belov NA, Glazoff MV. Chapter two—Structure and microstructure of aluminum alloys in As-cast state. In: Casting Aluminum Alloys. Amsterdam: Elsevier; 2007. p. 95-182 ISBN 9780080453705

[8] Callister WD. Materials science and engineering: An introduction (2nd edition). Materials and Design. 1991;**12**:59

[9] Votano J, Parham M, Hall L. Hanbook of Aluminum: Volume 2: Alloy Production and Material Manufacturing; John Wiley & Sons, Inc., United States. 2004. p. 1-731

[10] Baldwin W. Metallography and Microstructures. USA: ASM International; 2004. p. 2733

[11] Mackenzie DS. Handbook of Aluminum; Marcel Dekker, Inc., New York. 2003. DOI: 10.1201/9780203912607

[12] Zolotorevsky VS, Belov NA, Glazoff MV. Structure and Microstructure of Aluminum Alloys in As-Cast State, Amsterdam, The Netherlands: Elsevier, 2007

[13] Langdon TG. Twenty-five years of ultrafine-grained materials: Achieving exceptional properties through grain refinement. Acta Materialia. 2013;**61**:7035-7059

[14] Fukuda Y, Oh-ishi K, Furukawa M, Horita Z, Langdon TG. The application of equal-channel angular pressing to an aluminum single crystal. Acta Materialia. 2004;**52**:1387-1395

[15] Valiev RZ, Estrin Y, Horita Z, Langdon TG, Zehetbauer MJ, Zhu Y. Producing bulk ultrafine-grained materials by severe plastic deformation: Ten years later. JOM. 2016; **68**:1216-1226. DOI: 10.1007/s11837-016-1820-6

[16] Furukawa M, Horita Z, Nemoto M, Langdon TG. Review: Processing of metals by equal-channel angular pressing. Journal of Materials Science. 2001;**36**:2835-2843

[17] Liu MP, Roven HJ, Murashkin MY, Valiev RZ, Kilmametov A, Zhang Z, Yu Y. Structure and mechanical properties of nanostructured Al-Mg alloys processed by severe plastic deformation. Journal of Materials Science. 2013;**48**:4681-4688. DOI: 10.1007/s10853-012-7133-4

[18] Furukawa M, Horita Z, Nemoto M, Langdon TG. The use of severe plastic deformation for microstructural control. Materials Science and Engineering A. 2002;**324**:82-89

[19] Sabirov I, Murashkin MY, Valiev RZ. Nanostructured aluminium alloys produced by severe plastic deformation: New horizons in development. Materials Science and Engineering A. 2013;**560**:1-24

[20] Kawasaki M, Ahn B, Kumar P, Il Jang J, Langdon TG. Nano- and micro-mechanical properties of ultrafine-grained materials processed by severe plastic deformation techniques. Advanced Engineering Materials. 2017;**19**:1-17

[21] Lee BH, Kim SH, Park JH, Kim HW, Lee JC. Role of Mg in simultaneously improving the strength and ductility of Al-Mg alloys. Materials Science and Engineering A. 2016;**657**: 115-122

[22] Vinogradov A, Nagasaki S, Patlan V, Kitagawa K, Kawazoe M. Fatigue properties of 5056 Al-Mg alloy produced by equal-channel angular pressing. Nanostructured Materials. 1999;**11**:925-934

[23] Meng C, Zhang D, Cui H, Zhuang L, Zhang J. Mechanical properties, intergranular corrosion behavior and microstructure of Zn modified Al-Mg alloys. Journal of Alloys and Compounds. 2014;**617**:925-932

[24] Nakayama K, Tsuruta H, Koyama Y. Formation of giant atomic clusters in the β-Samson (β-Al$_3$Mg$_2$) phase of the Al-Mg alloy system. Acta Materialia. 2017;**128**:249-257

[25] Sato T, Kojima Y, Takahashi T. Modulated structures and GP zones in Al-Mg alloys. Metallurgical Transactions A. 1982;**13**:1373-1378

[26] Bouchear M, Hamana D, Laoui T. GP zones and precipitatemorphology in aged Al-Mg alloys. Philosophical Magazine A. 1996;**73**:1733-1740

[27] Starink MJ, Zahra AM. β′ and β precipitation in an Al-Mg alloy studied by DSC and TEM. Acta Materialia. 1998;**46**:3381-3397

[28] Starink MJ, Zahra A. The kinetics of isothermal β precipitation in Al-Mg alloys. Journal of Materials Science. 1999;**34**:1117-1127

[29] Hamana D, Bouchear M, Betrouche M, Derafa A, Rokhmanov NY. Comparative study of formation and transformation of transition phases in Al-12 wt.%Mg alloy. Journal of Alloys and Compounds. 2001;**320**:93-102

[30] Goswami R, Spanos G, Pao PS, Holtz RL. Precipitation behavior of the β phase in Al-5083. Materials Science and Engineering A. 2010;**527**:1089-1095

[31] Yi G, Littrell KC, Poplawsky JD, Cullen DA, Sundberg E, Free ML. Characterization of the effects of different tempers and aging temperatures on the precipitation behavior of Al-Mg (5.25 at.%)-Mn alloys. Materials and Design. 2016;**118** Submitted

[32] Król M, Tański T, Snopiński P, Tomiczek B. Structure and properties of aluminium– magnesium casting alloys after heat treatment. Journal of Thermal Analysis and Calo- rimetry. 2017;**127**:299-308. DOI: 10.1007/s10973-016-5845-4

[33] Tański T, Snopiński P, Borek W. Strength and structure of AlMg3 alloy after ECAP and post-ECAP processing Materials and Manufacturing Processes. 2017;**32**(12)

[34] Tański T, Snopiński P, Borek W. Strength and structure of AlMg3 alloy after ECAP and post-ECAP processing. Materials and Manufacturing Processes. n.d.:1-7

[35] Tański T, Snopiński P, Pakieła W. Structure and properties of ultra fine grained alumin- ium alloys after laser surface treatment. Materialwissenschaft und Werkstofftechnik. 2016;**47**:419-427. DOI: 10.1002/mawe.201600517

[36] Tański T, Snopiński P, Hilser O. Microstructure and mechanical properties of two binary Al-Mg alloys deformed using equal channel angular pressing. Materialwissenschaft und Werkstofftechnik. 2017;**48**:439-446. DOI: 10.1002/mawe.201700020